

## Thermodynamics of the Spin Luttinger Liquid in a Model Ladder Material

Ch. Rüegg,<sup>1</sup> K. Kiefer,<sup>2</sup> B. Thielemann,<sup>3</sup> D. F. McMorrow,<sup>1</sup> V. Zapf,<sup>4</sup> B. Normand,<sup>5</sup> M. B. Zvonarev,<sup>6</sup> P. Bouillot,<sup>6</sup> C. Kollath,<sup>7</sup> T. Giamarchi,<sup>6</sup> S. Capponi,<sup>8,9</sup> D. Poilblanc,<sup>9,8</sup> D. Biner,<sup>10</sup> and K. W. Krämer<sup>10</sup>

<sup>1</sup>*London Centre for Nanotechnology and Department of Physics and Astronomy, University College London, London WC1E 6BT, United Kingdom*

<sup>2</sup>*BENSC, Helmholtz Centre Berlin for Materials and Energy, D-14109 Berlin, Germany*

<sup>3</sup>*Laboratory for Neutron Scattering, ETH Zurich and Paul Scherrer Institute, CH-5232 Villigen PSI, Switzerland*

<sup>4</sup>*NHMFL, Los Alamos National Laboratory, Los Alamos, New Mexico 87545, USA*

<sup>5</sup>*Institute for Theoretical Physics, Ecole Polytechnique Fédérale de Lausanne, CH-1015 Lausanne, Switzerland*

<sup>6</sup>*DPMC-MaNEP, Université de Genève, CH-1211 Geneva 4, Switzerland*

<sup>7</sup>*Centre de Physique Théorique, École Polytechnique, CNRS, 91128 Palaiseau, France*

<sup>8</sup>*Université de Toulouse, UPS, Laboratoire de Physique Théorique, IRSAMC, F-31062 Toulouse, France*

<sup>9</sup>*CNRS, UMR 5152, F-31062 Toulouse, France*

<sup>10</sup>*Department of Chemistry and Biochemistry, University of Bern, CH-3000 Bern 9, Switzerland*

(Received 19 August 2008; revised manuscript received 24 October 2008; published 10 December 2008)

The phase diagram in temperature and magnetic field of the metal-organic, two-leg, spin-ladder compound  $(\text{C}_5\text{H}_{12}\text{N})_2\text{CuBr}_4$  is studied by measurements of the specific heat and the magnetocaloric effect. We demonstrate the presence of an extended spin Luttinger-liquid phase between two field-induced quantum critical points and over a broad range of temperature. Based on an ideal spin-ladder Hamiltonian, comprehensive numerical modeling of the ladder specific heat yields excellent quantitative agreement with the experimental data across the entire phase diagram.

DOI: 10.1103/PhysRevLett.101.247202

PACS numbers: 75.10.Jm, 75.40.Cx, 75.40.Mg

Quantum spin systems display a remarkable diversity of fascinating physical behavior. This is especially true for systems such as spin ladders, which have a gapped or a gapless ground state, respectively, for an even or an odd number of ladder legs [1]. For two-leg ladders, and in general for any even leg number, quantum phase transitions (QPTs) between gapped and gapless phases can be driven by an external magnetic field. While these QPTs are generic in quantum magnets [2], the nature of the gapless phase depends crucially on the dimensionality of the spin system. In two and higher dimensions, a quantum critical point (QCP) separates the low-field, quantum disordered (QD) phase, with gapped triplet excitations, from a gapless phase with long-range antiferromagnetic (AF) order, which can be well described as a Bose-Einstein condensate (BEC) of magnons [2–4].

By contrast, for one-dimensional (1D) systems such as ladders, both long-ranged magnetic order and BEC are precluded due to phase fluctuations. In addition, spin excitations are best viewed as interacting fermions, whereas a bosonic representation pertains in higher dimensions. The physics of the gapless phase in 1D is thus fundamentally different. It is a (spin) Luttinger liquid (LL) [5], and is a key component of the rich phase diagram presented in Fig. 1 [3,6–9]. In the LL, the spectrum is gapless with algebraically decaying spin correlations. Because there is no finite order parameter, the LL regime is reached from the high-temperature, classical regime through a crossover rather than a phase transition. Nevertheless, clear manifestations of LL behavior are expected not only in the corre-

lation functions but also in thermodynamic quantities such as the magnetization and specific heat.

However, materials in which to explore such effects are rather rare. Investigations of the spin excitations and thermodynamic properties of ladder compounds have to date been performed primarily on copper oxides. In these materials, the exchange interactions are typically some hundreds of meV, and thus the phases are not easily controlled by a magnetic field. Candidate 1D materials in which thermodynamic properties have been studied around the QPT include the bond-alternating  $S = 1/2$  and  $S = 1$  chains  $\text{F}_5\text{PNN}$  [10] and NTEMP [11], the  $S = 1$  Haldane system NDMAP [12,13], and the  $S = 1/2$  system  $\text{CuHpCl}$  [14], which was for some time considered to be a spin ladder [15]. While measurements in these materials show indications of LL behavior in parts of the field-temperature phase diagram, their magnetic properties are influenced in large part by the presence of significant single-ion anisotropy and/or three-dimensional (3D) interactions between the chains, which tend to dominate the low-temperature specific heat at all fields [16]. Hence we have pursued the search for materials suitable to study the intrinsic spin LL physics by seeking those showing, at minimum, a clear separation of energy (temperature) scales between 1D and 3D interactions.

Here we present the results of thermodynamic measurements on a prototypical two-leg ladder material, the metal-organic compound piperidinium copper bromide  $(\text{C}_5\text{H}_{12}\text{N})_2\text{CuBr}_4$  [17–22], where all of the phases of interest can be accessed, as summarized in Fig. 1. In particular,

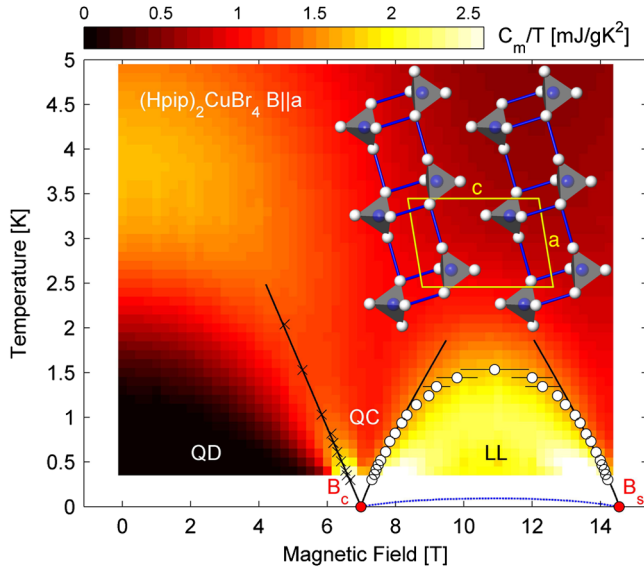


FIG. 1 (color online). Field-temperature phase diagram of the spin-ladder compound  $(\text{Hpip})_2\text{CuBr}_4$ , showing quantum disordered (QD), quantum critical (QC), and spin Luttinger-liquid (LL) phases. QCPs occur at  $B_c$  (closing of spin triplet gap  $\Delta$ ) and  $B_s$  (spin system fully polarized). The contour plot shows the magnetic specific heat as  $C_m(T, B)/T$ . Local maxima from the reduction of the triplet gap by the Zeeman effect are indicated by crosses. Circles denote the LL crossover based on measurements of the magnetocaloric effect [Fig. 4], black lines are fits to extract the critical fields, and the dashed blue line indicates the onset of long-ranged order below 100 mK [21,22]. Inset: lattice structure of  $(\text{Hpip})_2\text{CuBr}_4$  in projection along the  $b$  axis, with Cu atoms blue and Br white.

we find an extended region in the phase diagram, between 0.1 K and 1.5 K, where a spin LL is observed. We demonstrate that the crossover into the LL is signaled by clear features in both the specific heat and the magnetization. In the gapless spin LL, the magnetic specific heat is linear at low temperatures. Its field- and temperature-dependence are in excellent agreement with numerical calculations involving no free parameters. This demonstrates that the material is very accurately described by a minimal spin-ladder Hamiltonian.

High-quality single crystals of  $(\text{C}_5\text{H}_{12}\text{N})_2\text{CuBr}_4$ , abbreviated  $(\text{Hpip})_2\text{CuBr}_4$  in the following, were grown from solution. In this material, the  $S = 1/2$  magnetic moments of the  $\text{Cu}^{2+}$  ions are arranged in a ladderlike structure along the  $a$  axis [Fig. 1, inset]. The rungs ( $J_r$ ) of this ladder are formed by two equivalent Cu-Br-Br-Cu superexchange paths with a center of inversion symmetry [16], while the legs ( $J_l$ ) involve one similar but longer interaction path. The ladder units  $(\text{Cu}_2\text{Br}_8)^{4-}$  are well separated by the organic  $(\text{C}_5\text{H}_{12}\text{N})^+$  cations, which contribute only very little to the electronic properties of the host structure, and hence any magnetic exchange between ladders ( $J'$ ) is expected to be small. Direct measurements of these interactions,  $J_r = 12.9(2)$  K,  $J_l = 3.3(3)$  K, and  $J' < 100$  mK, based on inelastic neutron scattering experiments [23],

are in very close agreement with the values extracted from magnetostriction [20] and nuclear magnetic resonance (NMR) [21] measurements.

The specific heat and magnetocaloric effect (MCE) were measured on a purpose-built calorimeter at the Helmholtz Centre Berlin (Laboratory for Magnetic Measurements at BENSC), using single crystals of masses 4.78 mg and 9.69 mg in the respective temperature and field ranges 0.3 K to 15 K and 0 T to 14.5 T. The field was applied parallel to the crystallographic  $a$ -axis, a geometry in which we obtained the values  $B_c = 6.99(5)$  T and  $B_s = 14.4(1)$  T for the two QCPs [Fig. 1]. The specific heat was extracted from a quasiadiabatic relaxation technique and, using the same setup, the MCE was recorded with a sweep rate of 0.05 T per minute.

In Fig. 1 the magnetic component of the specific heat  $C_m/T$  of  $(\text{Hpip})_2\text{CuBr}_4$  is presented across the entire phase diagram. It shows clearly three distinct regimes: QD, quantum critical (QC), and spin LL. The contour plot was obtained from 27 scans in field and temperature, after subtraction of a field-independent lattice contribution  $C_l(T)$  and of a small nuclear term, which both are determined from a simultaneous fit to all available data.

In Fig. 2(a)–2(d) we show individual measurements of the total and the magnetic specific heat, respectively  $C_{\text{tot}}(T)$  and  $C_m(T, B)$ . In the QD regime,  $B \leq B_c$ ,  $C_m$  shows a single peak at approximately 5 K [Fig. 2(b)]. This peak is attributable to the triplet excitations of the ladder, and is exponentially activated at lower temperatures

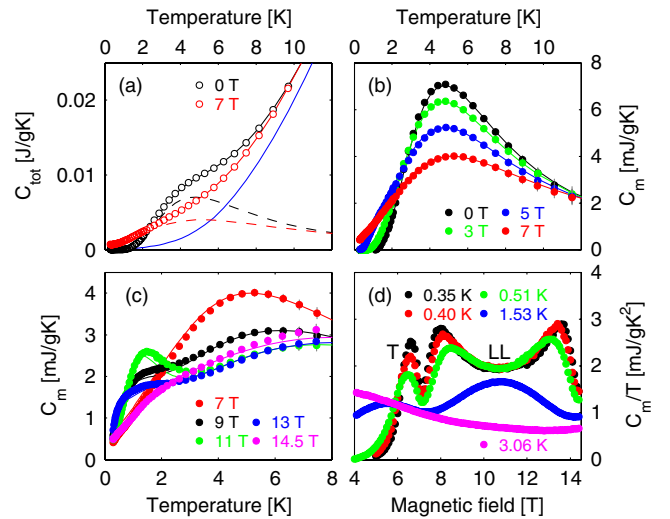


FIG. 2 (color online). (a) Measured total specific heat  $C_{\text{tot}}(T)$  at fixed magnetic field. Solid (dashed) lines are based on fits to the data before (after) background subtraction. The blue line indicates the uniform, nonmagnetic background. (b) Magnetic specific heat  $C_m(T, B)$  for  $B \leq B_c$ , and (c)  $B_c \leq B \leq B_s$ . Lines in (a)–(c) show  $C_m^{\text{ED}}$ , and are based on ED and DMRG calculations, as explained in the text. (d)  $C_m(T, B)/T$  measured at fixed temperature. The region with linear temperature dependence of the specific heat is indicated by LL, while T marks the peak due to the softening triplet.

due to the presence of the spin gap  $\Delta$  [24]. With increasing field, the gap is reduced by the Zeeman effect ( $\Delta \rightarrow \Delta - g\mu_B B$ ). Field scans such as those in Fig. 2(d) show most clearly the reduction of the gap and are used to extract the critical field  $B_c$  in Fig. 1, yielding very good agreement with determinations by complementary experimental techniques [18–22].

The specific heat changes dramatically for fields  $B > B_c$ , which we explain by the formation of the LL phase [Fig. 2(c)]. While at high temperature  $C_m$  is dominated by the (gapped)  $S_z = 0$  triplet states, at low temperature an additional peak develops. Below this peak, the temperature dependence remains linear up to  $B = B_s \approx 14.5$  T, with a field-dependent slope. The linearity of  $C_m$  is demonstrated in Fig. 2(d). For fields near the maximum of the LL dome, the ratio  $C_m/T$  measured at different temperatures collapses onto the same curve. This temperature dependence is consistent with the presence of gapless spinon excitations with a finite velocity  $u$ , its slope being inversely proportional to  $u$  [5]. The first peak thus occurs when the temperature is large enough to probe deviations from this linear regime. It can be taken as an estimate of the crossover to enter the LL, and is visible in Fig. 1 for  $B_c < B < B_s$ . The field dependence of  $C_m$  is almost symmetric about  $(B_c + B_s)/2 \approx 10.7$  T. In the strong-coupling limit,  $J_r/J_l \gg 1$ , perfect symmetry would be expected due to the exact particle-hole symmetry of the XXZ chain in a field [14,25]. Here we observe clear deviations characteristic of the underlying ladder structure. Similar effects are also visible in spin correlation functions and in the low-temperature phase diagram, which can be measured by NMR [21] and neutron scattering [22].

At  $B > B_s$ , the specific heat becomes exponentially activated again due to the opening of a field-dependent spin gap in the fully saturated phase. However, this regime is close to the limit of our experimental window, and so the high-field phase is not investigated further here.

The experimental data have been compared with several theoretical calculations, and the agreement is remarkable (Fig. 2). Numerical results were obtained by exact diagonalization (ED) and by adaptive, time-dependent density-matrix renormalization-group (DMRG) calculations [26], both performed for a single ladder with  $J_r = 13$  K,  $J_r/J_l = 4$ , and  $g = 2.06$  (i.e., no free parameters). We stress that in both techniques it is important to retain a sufficient number of ladder states for a quantitative description of thermodynamic data. The DMRG calculations ( $2 \times 40$  spins) may be regarded as the definitive behavior of this model. In the ED calculations, the specific heat of even- (odd-)length ladders converges rapidly from above (below) to the infinite-size limit; thus finite-size effects are essentially removed here by taking an average between systems of  $2 \times 10$  and  $2 \times 11$  spins. The ED and DMRG results are indistinguishable both in the QD phase [Fig. 2(b)] and in the LL regime [Fig. 2(c)]. Slight deviations from the experimental data are found only close to the upper critical field  $B_s$  and at 11 T.

Some physical insight into the numerical results is afforded by two approximate treatments. A statistical ansatz (TTW) [24] developed for spin ladders, and shown previously to describe very accurately the thermal renormalization of triplet excitations in the 3D dimer system  $\text{TlCuCl}_3$  [27], uses the correct number of states but applies their hard-core constraint only globally. In the spin ladder, this approximation underestimates the local energy of the excited states, leading to a systematic shift of weight to lower energies as  $B \rightarrow B_c$  [Fig. 3(a)]. A mapping of the lowest two modes of the ladder Hamiltonian onto an effective  $S = 1/2$  XXZ chain [14,25], whence thermodynamic quantities are computed exactly from the Bethe ansatz (BA), is very accurate for the low-energy physics at  $B > B_c$ , but cannot reproduce the heat capacity at higher temperatures because of the missing triplet states ( $S_z = 0, -1$ ) [Fig. 3(b)]. We conclude that the thermodynamic properties of  $(\text{Hpip})_2\text{CuBr}_4$  are described very accurately by a model of a single two-leg ladder, and that comprehensive measurements of the specific heat identify an extended LL regime.

We turn now to a different observable, the uniform magnetization ( $M$ ), which is notoriously difficult to measure at temperatures below 1.5 K. Very precise measurements can be obtained by NMR [21], but here we use an alternative method to probe the crossover to the LL. We determine the derivative of the magnetization with respect to temperature using the relation  $(\delta Q/\delta B)/T = -(\partial M/\partial T)|_B$ , where  $\delta Q$  is the amount of heat generated or absorbed by the sample for a field change  $\delta B$  due to the MCE. Figure 4 shows both representative  $(\delta Q/\delta B)/T$ -traces (corrected for a small base-line drift at higher temperatures) and a contour plot of all available data, presenting directly  $\partial M/\partial T$ . In the free-fermion model, which is an excellent qualitative description of spins near the QCP in 1D [5], and in more refined approaches [8,9,28], the magnetization has a minimum or maximum as a function of temperature ( $\partial M/\partial T = 0$ ). These extrema occur when the temperature matches the chemical potential, and thus provide another determination of the crossover temperature for the LL phase. The extracted phase boundary and the positions of the peaks in the

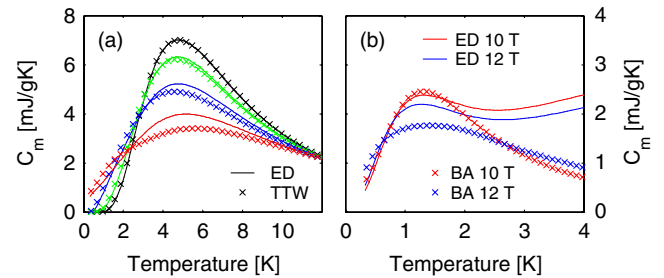


FIG. 3 (color online). Comparison of calculated ladder specific heat. (a) ED vs TTW for magnetic-field values  $B \leq B_c$  [as in Fig. 2(b)]. (b) ED vs BA for some magnetic-field values  $B > B_c$  [cf. Fig. 2(c)].

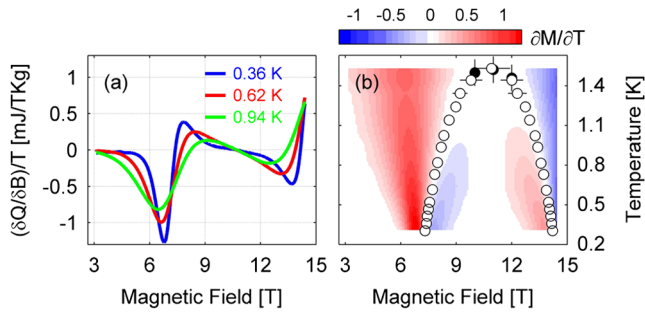


FIG. 4 (color online). Magnetocaloric effect in  $(\text{Hpip})_2\text{CuBr}_4$ . (a) Heat-flow  $\delta Q$  to and from the sample as a function of magnetic field divided by temperature,  $(\delta Q/\delta B)/T$ . (b) Contour plot of  $\partial M/\partial T$  as a function of field and temperature. White circles denote the phase boundary derived from  $\partial M/\partial T = 0$  (see also Fig. 1), while black circles are maxima in the specific heat,  $\partial C_m/\partial T = 0$ , obtained at fixed field.

specific heat agree well within expectations, as demonstrated by the solid symbols in Fig. 4(b).

The structures present here in the magnetization and specific heat differ markedly from those occurring when there is a BEC. In that case, because a real phase transition occurs, the specific heat diverges with a  $\lambda$ -type anomaly. Such a shape has been observed at BEC transitions in higher-dimensional materials such as  $\text{BaCuSi}_2\text{O}_6$  [29]. At the same temperature the magnetization develops a minimum, but with a cusplike structure [3], which has been observed in  $\text{TlCuCl}_3$  [4]. For 1D spin ladders, the magnetization minimum and the specific-heat peak have a different origin: they correspond to the crossover to the LL regime. Thus there is no divergence in the specific heat and the magnetization minimum is analytic, reflecting the absence of a phase transition; the temperatures of the two features, although similar, are not identical. For  $(\text{Hpip})_2\text{CuBr}_4$ , a real phase transition of BEC type does occur at a much lower temperature,  $T_N \approx 100$  mK (Fig. 1, [21,22]), due to a 3D coupling of the ladders.

In summary, we have measured the specific heat and magnetocaloric effect in the metal-organic, two-leg spin ladder  $(\text{C}_5\text{H}_{12}\text{N})_2\text{CuBr}_4$ . The excellent low-dimensionality and optimal energy scale of the exchange interactions make this material unique, and allow a detailed investigation of the phase diagram in temperature and in fields up to magnetic saturation for the quantum spin ladder. We find an extended region of spin Luttinger-liquid behavior over at least 1 order of magnitude in temperature, lying clearly above any three-dimensional physics triggered by residual interladder interactions. The high-precision experimental data have been analyzed using the most advanced exact diagonalization and density-matrix renormalization-group techniques to calculate thermodynamic quantities for all of the phases (i.e., across two quantum critical points). From the direct and parameter-free fit of the experimental and numerical results, we conclude that  $(\text{C}_5\text{H}_{12}\text{N})_2\text{CuBr}_4$  is remarkably well described by a minimal spin-ladder

Hamiltonian, with other possible effects (frustrated interactions, Dzyaloshinskii-Moriya terms, lattice coupling) being very small. Hence the material offers unprecedented opportunities to investigate the intrinsic physics of low-dimensional quantum systems.

We are grateful to C. Berthier and F. Essler for helpful discussions. This work was supported by the Royal Society, EPSRC, the Wolfson Foundation, the network “Triangle de la Physique”, the Swiss National Science Foundation through the NCCR MaNEP and Division II, and the French National Council (ANR). S.C. thanks Calmip (Toulouse) for computing time.

- [1] E. Dagotto and T.M. Rice, *Science* **271**, 618 (1996).
- [2] T. Giamarchi, Ch. Rüegg, and O. Tchernyshyov, *Nature Phys.* **4**, 198 (2008).
- [3] T. Giamarchi and A.M. Tsvelik, *Phys. Rev. B* **59**, 11 398 (1999).
- [4] T. Nikuni, M. Oshikawa, A. Oosawa, and H. Tanaka, *Phys. Rev. Lett.* **84**, 5868 (2000).
- [5] T. Giamarchi, *Quantum Physics in One Dimension* (Oxford University Press, New York, 2004).
- [6] S. Sachdev, T. Senthil, and R. Shankar, *Phys. Rev. B* **50**, 258 (1994).
- [7] A. Furusaki and S.C. Zhang, *Phys. Rev. B* **60**, 1175 (1999).
- [8] X. Wang and L. Yu, *Phys. Rev. Lett.* **84**, 5399 (2000).
- [9] S. Wessel, M. Olshanii, and S. Haas, *Phys. Rev. Lett.* **87**, 206407 (2001).
- [10] Y. Yoshida *et al.*, *Phys. Rev. Lett.* **94**, 037203 (2005).
- [11] M. Hagiwara *et al.*, *Phys. Rev. Lett.* **96**, 147203 (2006).
- [12] Z. Honda, K. Katsumata, Y. Nishiyama, and I. Harada, *Phys. Rev. B* **63**, 064420 (2001).
- [13] Y. Chen *et al.*, *Phys. Rev. Lett.* **86**, 1618 (2001).
- [14] G. Chaboussant *et al.*, *Eur. Phys. J. B* **6**, 167 (1998).
- [15] M.B. Stone *et al.*, *Phys. Rev. B* **65**, 064423 (2002).
- [16] In the absence of inversion symmetry, Dzyaloshinskii-Moriya interactions may also play an important role [S. Capponi and D. Poilblanc, *Phys. Rev. B* **75**, 092406 (2007)].
- [17] B.R. Patyal, B.L. Scott, and R.D. Willett, *Phys. Rev. B* **41**, 1657 (1990).
- [18] B.C. Watson *et al.*, *Phys. Rev. Lett.* **86**, 5168 (2001).
- [19] T. Lorenz *et al.*, *Phys. Rev. Lett.* **100**, 067208 (2008).
- [20] F. Anfuso *et al.*, *Phys. Rev. B* **77**, 235113 (2008).
- [21] M. Klanjsek *et al.*, *Phys. Rev. Lett.* **101**, 137207 (2008).
- [22] B. Thielemann *et al.*, arXiv:0809.0440v2.
- [23] B. Thielemann *et al.* (unpublished).
- [24] M. Troyer, H. Tsunetsugu, and D. Würtz, *Phys. Rev. B* **50**, 13 515 (1994).
- [25] K. Totsuka, *Phys. Rev. B* **57**, 3454 (1998); F. Mila, *Eur. Phys. J. B* **6**, 201 (1998).
- [26] A.E. Feiguin and S.R. White, *Phys. Rev. B* **72**, 220401 (2005).
- [27] Ch. Rüegg *et al.*, *Phys. Rev. Lett.* **95**, 267201 (2005).
- [28] Y. Maeda, C. Hotta, and M. Oshikawa, *Phys. Rev. Lett.* **99**, 057205 (2007).
- [29] M. Jaime *et al.*, *Phys. Rev. Lett.* **93**, 087203 (2004).